Structure and Toxicity Characterization of Alkyl Hydroxylated Metabolites of 6PPD-Q

Pranav Nair[a,#], Holly Barrett[a,#], Kaylin Tanoto[a], Linna Xie[a], Jianxian Sun[a], Diwen Yang[a], Han Yao[a], Datong Song[a,*], Hui Peng[*a,b,c]

[a] Department of Chemistry, University of Toronto, Toronto, ON M5S 3H6, Canada
[b] School of the Environment, University of Toronto, Toronto, ON M5S 3J1, Canada
[c] Structural Genomics Consortium (SGC), University of Toronto, Toronto, ON M5S 3H6, Canada

*Corresponding author: **Datong Song**, e-mail: d.song@utoronto.ca; **Hui Peng**, e-mail: hui.peng@utoronto.ca, Department of Chemistry, University of Toronto, Toronto, Ontario, M5S3H6, Canada.

Abstract

Distinct from other nontoxic PPD quinones, 6PPD-Q was recently discovered to be regioselectively metabolized to alkyl hydroxylated metabolites (alkyl-OH-6PPD-Q) in rainbow trout. It remains unknown whether the unique alkyl-OH-6PPD-Q might contribute to the toxicity of 6PPD-Q. To test this, we herein synthesized chemical standards of alkyl-OH-6PPD-Q isomers and investigated their metabolic formation mechanism and toxicity. The predominant alkyl-OH-6PPD-Q was confirmed to be hydroxylated on the C_4 tertiary carbon (C_4-OH-6PPD-Q). The formation of C_4-OH-6PPD-Q was only observed in microsomal, but not cytosolic fractions of rainbow trout (*O. mykiss*) liver S9. A general CYP450 inhibitor fluoxetine inhibited the formation of hydroxylated metabolites of 6PPD-Q, supporting that CYP450 catalyzed the hydroxylation. This well-explained the compound- and regio-selective formation of C_4-OH-6PPD-Q, due to the weak C-H bond on the C_4 tertiary carbon. Surprisingly, while cytotoxicity was observed for 6PPD-Q and C_3-OH-6PPD-Q in a coho salmon (*O. kisutch*) embryo (CSE-119) cell line, no toxicity was observed for C_4-OH-6PPD-Q. To further confirm this under physiologically relevant conditions, we fractionated 6PPD-Q metabolites formed in the liver microsome of rainbow trout. Cytotoxicity was observed for the fraction of 6PPD-Q, but not the fraction of C_4-OH-6PPD-Q. In summary, this study highlighted the C_4 tertiary carbon as the key moiety for both metabolism and toxicity of 6PPD-Q, and confirmed that alkyl hydroxylation is a detoxification pathway for 6PPD-Q.

Keywords: Rainbow trout; Coho Salmon; CYP450; Hydroxylated metabolites; Proteomics

Synopsis: The C_4 tertiary carbon of 6PPD-Q is important for its unique metabolism and toxicity. Alkyl hydroxylation by CYP450 seems to be a detoxification pathway for 6PPD-Q.

Introduction

A recent milestone study identified the ozonation product of *N*-(1,3-dimethylbutyl)-*N*′-phenyl-*p*-phenylenediamine (6PPD), *N*-(1,3-dimethylbutyl)-*N*′-phenyl-*p*-phenylenediamine-quinone (6PPD-Q), as the toxicant responsible for the acute mortality of coho salmon (*O. kisutch*).[1] 6PPD-Q exerts extreme aquatic toxicity in coho salmon with a median lethal concentration (LC_{50}) of 95 ng/L.[1,2] The discovery of this chemical has sparked a flurry of interest into 6PPD-Q from both environmental chemists and toxicologists. One major discovery has been the high interspecies variation in the toxicity of 6PPD-Q, as only members of the family *Salmonidae* appear to be sensitive to 6PPD-Q, but even within the family there is a substantial variation across species.[3–6] For instance, 6PPD-Q was found to be toxic to rainbow trout (*O. mykiss*) but not to arctic char (*S. alpinus*),[7] yet the toxicity mechanism has not been elucidated.

Recent studies from our group discovered the structurally selective toxicity of 6PPD-Q in rainbow trout, while toxicity was not observed for other PPD-Qs with very similar structures.[8] Correspondingly, a differential pattern in metabolism was observed across PPD-Qs in rainbow trout, where the most abundant metabolite formed for 6PPD-Q was hydroxylated on the alkyl side chain as opposed to the aromatic hydroxylation observed for the rest of the PPD-Qs. This alkyl hydroxylated metabolite was detected at an even higher abundance than native 6PPD-Q in rainbow trout fish tissue after 96 hours of exposure.[9] The formation of alkyl-OH-6PPD-Q was further confirmed in additional studies on rainbow trout, humans, and other species.[10–13] Bioactivation of xenobiotics is a common mechanism to cause toxicity, as exemplified by the stronger toxicity of hydroxylated metabolites compared to native polychlorinated biphenyls (PCBs).[14–18] The unique toxicity and regioselective hydroxylation of 6PPD-Q prompted the hypothesis that alkyl-OH-6PPD-Q rather than native 6PPD-Q might be the toxic species. Alternatively, alkyl-OH-6PPD-Q

might be a detoxification pathway for 6PPD-Q (see hypotheses in Figure 1A). It would be of great interest to examine the potential role of alkyl-OH-6PPD-Q in mediating the toxicity of 6PPD-Q. However, due to the lack of chemical standard, the identity or toxicity of alkyl-OH-6PPD-Q has not been examined.

In addition to toxicity, the enzymatic mechanism for the regioselective hydroxylation of 6PPD-Q on the alkyl side chain is also interesting. A recent study from the Brinkmann group suggested that CYP1A might catalyze the hydroxylation of 6PPD-Q in rainbow trout liver cells (RTL-W1), by using human CYP450 isozyme-specific inhibitors.[10] While this study provided important evidence on the potential role of CYP450 enzymes, it has been well established that CYP1A generally hydroxylates aromatic rings of xenobiotics.[19–23] Thus, this may not explain the chemical mechanism for the regioselective hydroxylation of 6PPD-Q on the alkyl side chain. An in-depth exploration of this mechanism is therefore important to understand the structure-related metabolism and toxicity of PPD-Q compounds.

Given the interest surrounding the alkyl-OH-6PPD-Q in both the toxicity and metabolism of 6PPD-Q, we endeavoured to 1) characterize the structure of alkyl-OH-6PPD-Q with synthesized chemical standards, 2) examine the formation of alkyl-OH-6PPD-Q using S9 and subcellular fractions of rainbow trout liver to understand the enzymatic mechanism, and 3) assess the *in vitro* toxicity of alkyl-OH-6PPD-Q using the coho salmon embryo (CSE-119) cell line. This is the first study to systematically characterize the structure, metabolism, and toxicity of alkyl-OH-6PPD-Q, which is crucial to understand the toxicity mechanism of 6PPD-Q.

Materials and Methods

Chemicals and Reagents. All chemical reagents were purchased from commercial vendors and used without further purification, unless otherwise specified. All reactions necessitating oxygen- or moisture-free conditions were conducted using oven-dried glassware under a nitrogen atmosphere. Reagent-grade solvents were used for all chemical reactions. HPLC-grade methanol and acetonitrile were purchased from EMD Chemicals (Gibbstown, NJ, United States). 6PPD-Q and d_5-6PPD-Q chemical standards were purchased from Toronto Research Chemicals (North York, ON, Canada). The fluoxetine chemical standard and NADPH tetrasodium salt (98 %) were purchased from Sigma (Oakville, ON, Canada). Phosphate buffered saline (PBS) tablets were purchased from Froggabio (Concord, ON, Canada). Sodium cholate (SC), digitonin (Dig), and n-dodecyl-β-D-maltoside (DDM) detergents were purchased from Sigma (Oakville, ON, Canada). 2-amino-4-methylpentan-3-ol was purchased from Enamine (Monmouth Junction, NJ, United States).

Synthesis of Hydroxylated 6PPD-Qs. The synthesis of two alkyl-OH-6PPD-Q isomers was the primary synthetic focus of this work. The two isomers will henceforth be referred to as the C_3-alkyl-OH-6PPDQ and C_4-alkyl-OH-6PPDQ metabolites. The synthesis of the C_3-alkyl-OH-6PPDQ was achieved in 1 step via the adaptation of a previously reported synthetic protocol[24] and the use of the purchased α-amino alcohol, 2-amino-4-methylpentan-3-ol, to yield the desired compound, albeit at a poor yield (13%). The synthesis of the C_4-alkyl-OH-6PPDQ was completed in 3 steps, starting from the commercially available diacetone alcohol to prepare the β-amino alcohol, and then the subsequent substitution of mono-aniline substituted paraquinone to yield the second isomer. Both compounds necessitated the use of reverse phase (RP) – flash chromatography to purify. The purity of each chemical standard was confirmed via proton nuclear

magnetic resonance (^{1}H-NMR) and carbon-13 NMR (^{13}C-NMR) conducted on an Agilent DD2 500 MHz spectrometer with comparison to an internal standard (mesitylene). Purity was further validated by LC-HRMS analysis. Detailed synthetic procedures were provided in the *Supporting Information*.

Fish Tissue Collection and Preparation. Two each of rainbow trout and arctic char were kindly gifted by Ryan Hill and Mark Newell from the Centre for Innovative Aquaculture Production (Fleming College, Lindsay, ON, Canada) hatchery. All fish were sexually mature females weighing approximately 800 g. Fish were kept alive in oxygenated plastic bags during transport and were then anesthetized and dissected on ice immediately to avoid loss of enzyme activity, as per guidelines from Organisation for Economic Co-operation and Development (OECD) Test No. 319B.[25] The whole organs of each fish were excised with sterile stainless steel surgical scissors, transferred to Eppendorf tubes, flash-frozen on dry ice, and then stored immediately at -80 °C until further preparation.

S9 was prepared from various tissues (*i.e.*, liver, brain, gill, intestine) of both species via an adapted version of the OECD Test No. 319b guidelines.[25] Tissue was thawed on ice before being rinsed with ice cold phosphate buffer [0.08 M sodium phosphate, 0.02 M potassium phosphate; pH = 7.4]. Excess fluid was removed, and the tissue was minced with sterile stainless steel surgical scissors on ice. Approximately 0.2 g of tissue was transferred to a 2 mL Eppendorf tube, suspended in 800 µL ice cold phosphate buffer (4 mL_{buffer}/g_{tissue}), and homogenized with 10 strokes of a Fisher Scientific Powergen 125 (FTH-115) blade-type homogenizer on ice. Multiple replicates were prepared. Following this, the tissue was centrifuged at 9,000 g for 15 min at 4 °C, and the supernatant (tissue S9) was transferred to a new tube and stored at -80 °C until further preparation or use. To prepare microsomal or cytosolic sub-cellular fractions from the liver S9, we used an

adapted version of Dyer's method.[26,27] In brief, 800 µL of tissue S9 was transferred to an ultracentrifuge tube and suspended in 14.2 mL of ice-cold phosphate buffer. The S9 was ultracentrifuged at 100,000 g for 60 min at 4 °C. The supernatant (cytosolic fraction) was transferred to new tubes and stored at -80 °C until use. The pellet (microsome fraction) was then re-suspended in 2 mL of ice-cold phosphate buffer and stored at -80 °C until use. The total protein concentration of tissue S9, microsome, and cytosol fractions were determined by Bradford protein assay.

Fish S9, Microsome, and Cytosol Metabolism Experiments. For *in vitro* incubations of rainbow trout or arctic char S9, microsome, or cytosol, the reactions were performed in 0.05 M sodium phosphate buffer (pH 8.0) in the dark, using an adapted version of OECD Test No. 319B.[25] The reaction mixtures (250 µL) consisting of ~ 10 µL S9/microsome/cytosol (final reaction concentration = 0.15 µg/µL protein), 12 µL of a 10.5 mM NADPH stock solution, and 5 µL of a 5 mg/L 6PPD-Q stock solution and were incubated in 1.5 mL Eppendorf tubes. Incubations were carried out in triplicate in separate tubes at 20 °C to mimic physiological conditions, and 200 µL of ice-cold acetonitrile was added into each vial to terminate the reaction. Initially, the reaction was terminated after 0, 1, 5, and 24 h. It was then determined that sufficient metabolite was formed after 5 h (Figure S1), and therefore all subsequent reactions were performed for 5 h. Prior to instrument analysis, the reaction extracts were centrifuged for 10 min at 10,000 g, and 45 µL of each extract was transferred to an LC vial with 5 µL of 100 µg/L of d_5-6PPD-Q internal standard and vortexed to mix.

Metabolite Fractionation by HPLC. An incubation of rainbow trout microsome with 6PPD-Q was carried out using the conditions described above with minor modifications to increase the quantity of metabolite products. Namely, the reaction concentration of protein was increased to

0.5 mg/mL, and the concentration of 6PPD-Q in the reaction media was increased to 1 mg/L. The final extract was fractionated with an Agilent 1260 Infinity II HPLC (Agilent Technologies) with an C18 column (Accucore Vanquish, 50 mm × 2.1 mm, 1.5 μm; Thermo Scientific). Twenty microliters of extract was loaded onto the column. HPLC grade water with 1 % formic acid and and methanol with 1 % formic acid were used as mobile phases A and B, respectively, with a flow rate of 0.5 mL/min. The LC method was as follows: B was kept static at 5% from 0 to 2 min, increased to 100% from 2 to 11 min, kept static at 100% from 11 to 15 min, then returned to 5% from 15 to 16 min, and maintained at 5% until 20 min. The signal intensity was measured at 280 nm and 350 nm. Twenty fractions were collected at a time interval of 1 min from 1 to 20 min in microcentrifuge tubes. Fractions were dried by vacuum concentration (Savant SpeedVac; Thermo Scientific) and reconstituted in 50 μL of methanol.

Cell Culture and Toxicity Testing. Coho salmon embryo cells (CSE-119) were incubated at 20 ºC in culture media [Leibovitz's L-15 medium (Gibco) supplemented with 10% fetal bovine serum (Peak Serum, Inc.) and 10% penicillin-streptomycin (Cytiva HyClone)].[28] Toxicity was evaluated using alamarBlue or neutral red cell viability assays.[28,29] For the alamarBlue assay, resazurin sodium salt was dissolved in phosphate buffered saline (PBS) at a concentration of 0.30 mg/mL, which was passed through a sterilizing filter (0.22 μm) and stored at -20 °C in darkness until use. For the neutral red assay, a stock solution of neutral red dye was prepared in PBS at a concentration of 4 mg/mL and stored at room temperature in the dark. One day prior to use, neutral red media was prepared at a concentration of 40 μg/mL in culture media, incubated at 20 ºC overnight with shaking, and centrifuged at 10,000 g prior to cell dosing to remove any undissolved dye crystals. 24 hours before cell exposure, CSE-119 cells were seeded in a 96-well plate with a density of 10,000 cells/well in 100 μL of culture media. Exposure media was prepared fresh by dissolving

stock solutions of 6PPD-Q chemical standard or synthesized OH-6PPD-Qs (in acetonitrile) in fresh culture media. Culture media in 96-well plates was replaced with 100 µL of seven 3-fold serial diluted exposure media (0.34 to 250 µg/L). The percentage of acetonitrile in the culture media was less than 0.2 %, and acetonitrile at this percentage did not influence cell viability. For toxicity testing of metabolites extracted from fish liver microsome, both pre- and post-HPLC fractionation, the percentage of acetonitrile in the culture media was less than 1 %, which did not influence cell viability. There were 4 replicates for each concentration. For the alamarBlue assay, after 48 hours of exposure at 20 °C, 10 µL of cell viability reagent was added to each well in a dark room, then the cells were incubated for 4 h at 20°C in darkness. After that, fluorescence was recorded with excitation at 550 nm and emission at 600 nm by a Tecan Infinite 200 Pro M Plex microplate reader (Tecan Life Sciences, Switzerland). Cell viability was calculated as the measured fluorescence value at each well compared with that of the solvent control from the same plate. For the neutral red assay, after 48 hours of exposure at 20 °C, exposure media was removed from the cells and 100 µL of neutral red media was added to each well. The cells were incubated for 4 h at 20°C in darkness to allow for dye uptake via the lysosomes of viable cells, and then the neutral red media was removed. Following this, the cells were washed with 150 µL PBS per well, and 150 µL destaining solution (50 % ethanol, 49 % deionized water, 1 % glacial acetic acid) was added per well. The 96-well plate was shaken rapidly in a microtiter plate shaker for 10 minutes to form a homogenous solution in each well. After that, the optical density of each well was recorded by a Tecan Infinite 200 Pro M Plex microplate reader at 540 nm. Cell viability, expressed as a percentage of solvent controls, was then calculated.

LC-Orbitrap Analysis of Small Molecules. Chemical analysis was conducted with a Q-Exactive mass spectrometer equipped with a Vanquish UHPLC system (Thermo Fisher Scientific).

Separation was achieved with a C18 column (Accucore Vanquish, 50 mm × 2.1 mm, 1.5 μm; Thermo Scientific). The injection volume was 2 μL, with 1% formic acid in ultrapure water (A) and 1% formic acid in methanol (B) as the mobile phases. Initially, 5 % B was increased to 50 % from 0 to 2 min, then increased to 100 % at 6 min and held static for 7.5 min, followed by a decrease to initial conditions of 5 % B for 0.5 min, which was held for 1 min to allow for equilibration. The flow rate was 0.15 mL/min. The column and sample compartment temperatures were maintained at 40 and 4 °C, respectively. Data were acquired in full scan MS^1 and data-independent acquisition (DIA) MS^2 modes. Parameters for full scan MS^1 (100–900 m/z) switch mode were as follows: recorded at resolution R = 70 000 (at *m/z* 200) with a maximum of 3×10^6 ions collected within 100 ms. In both negative and positive modes, two DIA tandem MS (MS/MS) scans were established by covering the *m/z* ranges of 100 to 500 and 500 to 900, respectively. The DIA scan had an isolation window of 20 *m/z*. Mass spectrometric settings for both ESI (−) and ESI (+) modes were as follows: spray voltage of 3.0 kV; sheath gas flow rate of 30 L/h; auxiliary gas flow rate of 6 L/h; capillary temperature of 300 °C.

Shotgun Proteomics. Shotgun proteomics was used to profile the CYP450 enzymes across RT liver, brain, intestine, and gill tissue S9. The proteomics sample preparation was performed as outlined in previous studies.[30,31] S9 was digested with trypsin and the peptides were injected into an EASY-nanoLC 1200 UHPLC, operated under electrospray ionization, paired with a Q-Exactive H-X Orbitrap mass spectrometer (Thermo Fisher Scientific; Waltham, MA, USA). Samples were separated on an in-house packed C_{18} column (10 cm × 75 μm internal diameter, packed with 3 μm Luna C_{18} 100 Å reverse phase beads (Phenomemex; Torrance, CA, USA)). The nanoLC mobile phases were A) 0.1 % formic acid in water, and B) 0.1 % formic acid in 80:20 acetonitrile:water.

B was increased from 2 to 5 % for 1 min, gradually increased to 26 % for 89 min, increased to 100 % at 105 min, and held at 100 % for 15 min. The flow rate 300 nL min^{-1}.

Data-dependent acquisition (DDA) was used to detect the top 20 peptides. Full MS scan parameters were as follows: *m/z* range of 350 – 1400, resolution of 60,000 at *m/z* =200, AGC of 3 × 10^6. MS^2 scans held precursor ions 1.4 *m/z* windows and were accumulated for 20 ms or until the AGC target was reached.

Quality Assurance and Quality Control. For each batch of metabolism experiments, one blank sample and two forms of negative control were included. The blank was prepared as described above but without 6PPD-Q, which was replaced with an equivalent volume of buffer. Heat-inactivated S9 (heated at 100 ºC for 10 min) of rainbow trout or arctic char was used as a negative control.[25] An additional negative control with S9, microsome, or cytosol, but without NADPH, was also used. Triplicate experiments were performed for each treatment group to ensure the reproducibility and consistency of the potential metabolites. For the instrumental analyses, procedural blanks were incorporated with each batch of samples to monitor for potential background contamination. Injections of 6PPD-Q chemical standard were performed following every 10 sample injections to monitor for instrument stability, followed by an injection of MeOH to monitor for potential carryover. Quantification of 6PPD-Q and semi-quantification of metabolites was determined using the relative response against the d_5-6PPD-Q internal standard using calibration curves of 6PPD-Q. The recovery of 6PPD-Q in the metabolism incubation experiments at 5 hr was 98 ± 8 %. The method detection limit (MDL) of 6PPD-Q was calculated by a 99 % confidence level of y-intercept divided by the slope of the calibration curve and was 2.2 – 3.0 µg L^{-1} for the metabolism experiments. Proteomics cross-tissue experiments were performed in triplicate.

Data Analysis. Statistical analyses were performed using GraphPad Prism (v10.1.2, GraphPad Software Inc., San Diego, CA). All dose-response curves were fit using the nonlinear regression of log-transformed data *via* GraphPad Prism, and half-maximal effect concentration (EC_{50}) values were determined using the fitted curves. Raw proteomics data were analyzed using MaxQuant (version 2.4.10) and default parameters were used with a false discovery rate of 1 % with a list of common contaminants. The rainbow trout proteome was obtained from Uniprot and used to match extracted MS^2 spectra. Proteomics data were analyzed using GraphPad Prism. In cases where a peptide was below the limit of detection in one or two out of three replicates, it was assigned an intensity value of 1.5E04, which corresponded to the intensity of the lowest intensity peptide detected in the dataset divided by two. Raw MS files and their resulting MaxQuant output tables have been uploaded to the MassIVE repository and ProteomeXchange (MSV000096218). Analyzed proteomics evidence and protein groups data from MaxQuant, including annotated CYP450-related peptides, are provided as the supplementary excel files Supplementary Data 1 and Supplementary Data 2, respectively.

Results and Discussion

Synthesis and structure confirmation of alkyl-OH-6PPD-Q. While we previously identified an alkyl-OH-6PPD-Q metabolite in rainbow trout fish tissue after exposure to 6PPD-Q, we could not discern the exact position of hydroxylation on the alkyl side chain.[8] Upon inspection of the MS^2 spectrum of alkyl-OH-6PPD-Q, two characteristic MS^2 fragments of 241.0969 and 257.1284 suggested that the hydroxyl group was likely located at the C_3 or C_4 carbon position (Figure S2A). We therefore elected to focus on the synthesis of the C_3- and C_4-alkyl-OH-6PPD-Q isomers individually to confirm the position of hydroxylation. We started by synthesizing the C_3-alkyl-

OH-6PPD-Q isomer, largely because its starting material (the α-amino-alcohol 2-amino-4-methylpentan-3-ol) was commercially available. The synthesis was achieved in a single step via the substitution of 2-anilino-1,4-benzoquinone with 2-amino-4-methylpentan-3-ol (Figure 1B). Further details of the synthesis were described in Text S1. The identity and purity (> 90%) of the synthesized C_3-OH-6PPD-Q was characterized by LC-MS, NMR (Figures S3 – S5), and IR (Figure S6). However, when compared to the major alkyl-OH-6PPD-Q formed in rainbow trout fish tissues (retention time = 4.70 min), the retention time of the synthesized C_3-alkyl-OH-6PPD-Q (4.93 min) did not match (Figure 1C). The MS^2 spectrum of the synthesized standard further confirmed that C_3-alkyl-OH-6PPD-Q was not the major alkyl metabolite formed in rainbow trout as it did not possess diagnostic fragments at *m/z* 257.1283 and 241.0971 (Figure S2C). Instead, the C_3-OH-6PPD-Q standard possessed a unique fragment at *m/z* 243.1128, which corresponded to a minor alkyl-OH-6PPD-Q metabolite identified in the fish tissue extract that also elutes at 4.93 min. Due to the low concentration of this metabolite, we proceeded to focus on the predominant alkyl-OH-6PPD-Q metabolite at 4.70 min.

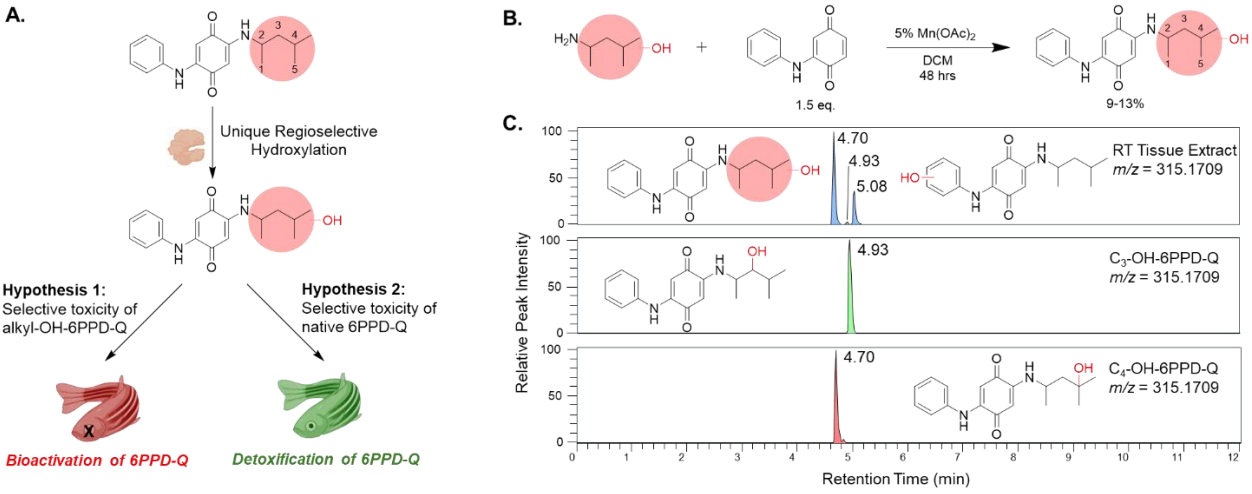

Figure 1. (A) The unique formation of alkyl-OH-6PPD-Q by an unknown enzyme might contribute to the toxicity of 6PPD-Q. (B) The synthetic route for the preparation of alkyl-OH-6PPD-Q isomers. (C) The chromatograms of alkyl-OH-6PPD-Q from rainbow trout (RT) tissue extracts (top), synthesized chemical standards of C_3-alkyl-OH-6PPD-Q (middle) and C_4-alkyl-

OH-6PPD-Q (bottom). The minor OH-6PPD-Q formed in fish tissue at the retention time of 4.93 min was confirmed to be C_3-alkyl-OH-6PPD-Q.

Starting from the commercially available diacetone alcohol, we were able to achieve the synthesis of C_4-alkyl-OH-6PPD-Q in 3 steps, and similarly characterized its identity and purity (> 90%) with LC-MS, NMR (Figures S7-9), and IR (Figure S10). Comparison of the LC trace of synthesized C_4-alkyl-OH-6PPD-Q with a tissue extract of 6PPD-Q-exposed rainbow trout revealed a common retention time (4.71 min; Figure 1B). Moreover, their MS^2 spectra contained common diagnostic fragments at *m/z* 241.0969 and 257.1284 (Figure S2A and S2D). Collectively, by using two synthesized chemical standards, we confirmed the predominant alkyl-OH-6PPD-Q formed in rainbow trout fish tissue as C_4-alkyl-OH-6PPD-Q.

Enzymatic mechanism for the regioselective formation of C4-alkyl-OH-6PPD-Q. After the confirmation of hydroxylation on the C_4 carbon, we proceeded to investigate the enzymatic mechanism for the regioselective hydroxylation of 6PPD-Q. To achieve this, we used liver S9 of rainbow trout as an *in vitro* model.[25,32–34] After the incubation of 6PPD-Q with liver S9 for 5 hours, C_4-alkyl-OH-6PPD-Q (retention time = 5.47 min) and aryl-OH-6PPD-Q (retention time = 6.02 min) were clearly detected (Figure 2A; MS^2 in Figure S2B). Similar formation of OH-6PPD-Qs was not observed in negative controls wherein liver S9 was heated deactivated. Additionally, the formation of OH-6PPD-Qs was not observed in the absence of NADPH, demonstrating that NADPH was an essential cofactor for the enzymatic reactions.

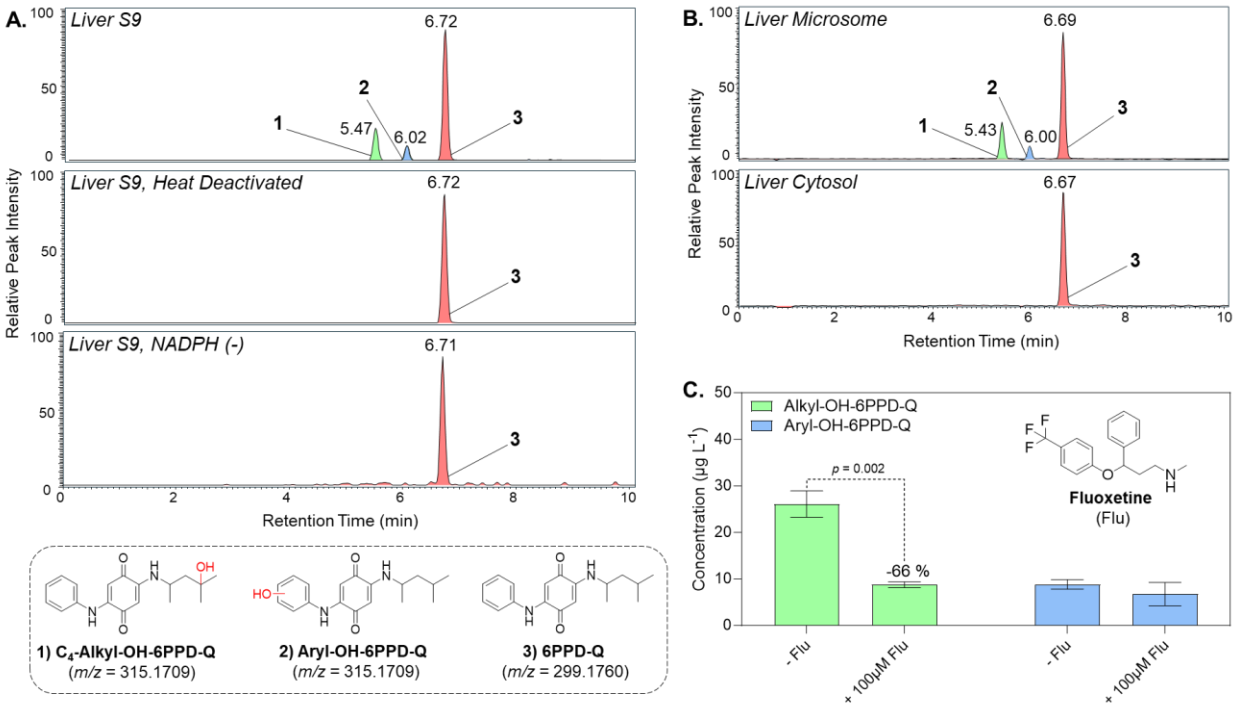

Figure 2. (A) C_4-alkyl- and aryl-OH-6PPD-Q metabolites were produced via incubation of 6PPD-Q in rainbow trout liver S9, but not in heat deactivated liver S9, or in the absence of NADPH (NADPH (-)). (B) C_4-alkyl- and aryl-OH-6PPD-Q metabolites were produced via incubation of 6PPD-Q in rainbow trout liver microsome, but not in liver cytosol. C) The production of the C_4-alkyl-OH-6PPD-Q metabolite was significantly inhibited by the introduction of 100 μM of the general CYP450 inhibitor fluoxetine (Flu) to rainbow trout liver microsomal incubation media.

We further isolated the microsomal and cytosolic fractions from liver S9 by using ultracentrifugation to examine the subcellular location of the catalytic enzymes. As shown in Figure 2B, formation of C_4-alkyl-OH-6PPD-Q and aryl-OH-6PPD-Q was observed in the microsomal fraction but not in the cytosolic fraction. The exclusive formation of OH-6PPD-Qs in the liver microsome indicated that the enzymes catalyzing the hydroxylation may belong to the CYP450 family, as it is well-known that CYP450 enzymes are located in microsome and catalyze the hydroxylation of xenobiotics.[35] To further confirm this, we co-incubated 6PPD-Q in microsome with fluoxetine (Flu; see structure in Figure 2), which has been benchmarked as a general CYP450 inhibitor in rainbow trout.[36] The co-incubation of 6PPD-Q with 100 μM of

fluoxetine in liver microsome significantly inhibited the production of the C_4-alkyl-OH-6PPD-Q metabolite by 66 ± 8 % (p = 0.002), while the production of the aryl-OH-6PPD-Q metabolite also appeared to be minorly inhibited (~23 %) albeit not to a statistically significant extent (Figure 2C). The more efficient inhibition of C_4-alkyl-OH-6PPD-Q by fluoxetine demonstrated that the two metabolites might be catalyzed by different CYP450 isozymes. The confirmation of CYP450 as the catalytic enzyme of 6PPD-Q hydroxylation was consistent with a recent study from the Brinkmann group which reported the decreased biotransformation of 6PPD-Q in a rainbow trout liver cell line (RTL-W1) upon co-incubation with certain CYP450 inhibitors.[10]

After confirmation of the role of CYP450, we then proceeded to identify the isozyme among the ~35 isozymes annotated in rainbow trout.[37] While the co-incubation of substrates with isozyme-specific CYP450 inhibitors has been widely used as an approach to pinpoint key isozymes in mammals such as humans, such an approach is infeasible in fish species (*i.e.*, rainbow trout) as they do not possess the same isozyme specificity.[38] We initially attempted to purify the CYP450 isozyme from the crude liver microsome of rainbow trout using size-exclusion chromatography, which required the solubilization of membrane-bound CYP450 enzymes with detergents, as reported in previous studies.[39–42] Unfortunately, despite months of effort, this biochemical strategy was unsuccessful as 80 – 99 % of enzyme activity was lost among the 5 different detergent conditions we selected based on previous CYP450 enzyme studies (Table S1, Figure S11).[39–42]

We then employed a completely different approach using shotgun proteomics since the genome sequence of rainbow trout has been well-defined.[37] To achieve this, we first incubated 6PPD-Q with S9 prepared from four different tissues including liver, brain, intestine, and gill. Not surprisingly, the highest formation of C_4-alkyl-OH-6PPD-Q and aryl-OH-6PPD-Q was detected from liver S9, while minor or no formation was observed in S9 from other tissues (Figure 3A).

This clearly demonstrated that the catalytic CYP450 isozyme was tissue-specifically expressed in liver. We then used shotgun proteomics to profile the tissue distribution of CYP450 isozymes. Across all four tissues, peptides associated with a total of 10 CYP450 isozymes were detected (CYP27A1, 2F2, 2F3, 2J2, 2K1, 2M1, 3A27, 3A30, 4B1, and 4V2; Figure 3B). The absence of CYP1A isozymes at a significant level was consistent with a previous study on the closely related salmonid species coho salmon (*O. kisutch)* wherein isozymes CYP450 2K1, 2M1, and 3A27 were found to be much more highly expressed in liver than CYP1A1.[43] These results did not align with a recent study suggesting CYP1A as the primary catalyzing enzyme of 6PPD-Q hydroxylation.[10] In that study, human CYP1A-specific inhibitors α-naphthoflavone (ANF) and quercitin were used, but these two inhibitors have been reported as non-specific towards CYP1A in rainbow trout.[44–46] Thus, CYP1A may not be the isozymes responsible for 6PPD-Q hydroxylation in rainbow trout.

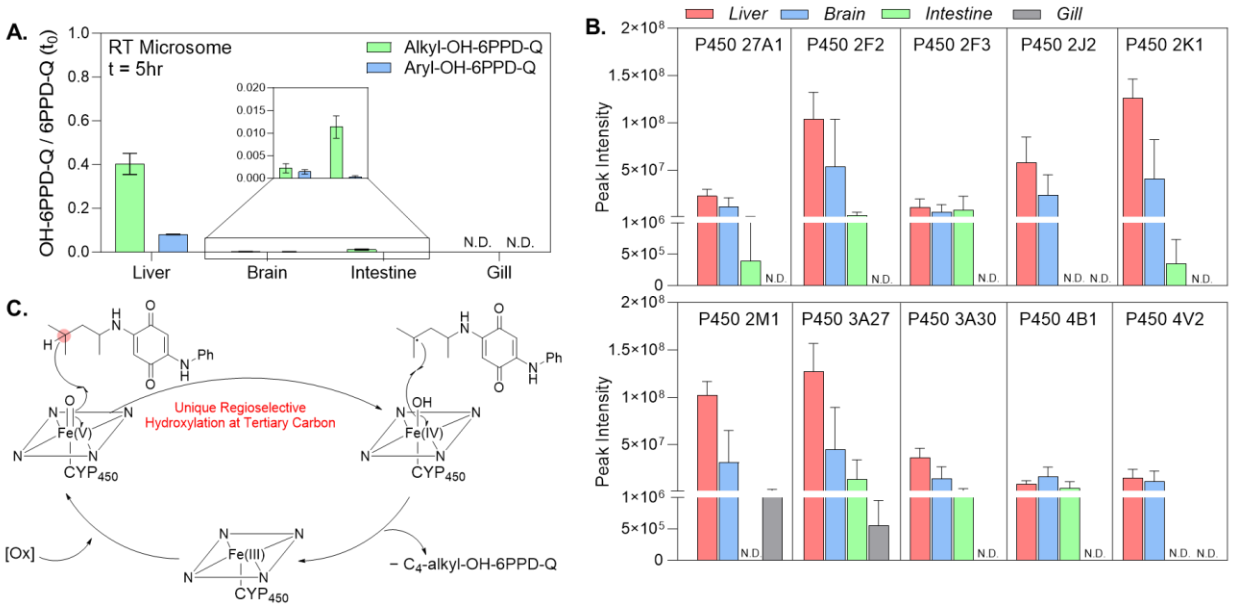

Figure 3. A) Tissue-specific differences in the production of Alkyl- and Aryl-OH-6PPD-Q metabolites in rainbow trout microsomal incubations. B) Cross-tissue proteomics analysis of CYP450 isozymes in rainbow trout S9. C) Mechanism for the regioselectivity of 6PPD-Q hydroxylation by a CYP450 enzyme. 'N.D.' denotes not detected.

Notably, distinct expression profiles of CYP450 isozymes were observed across tissues, with 10 detected in liver, 10 in brain, 7 in intestine, and 2 in gills. This provided an opportunity to correlate tissue-specific expression of CYP450 isozymes to the tissue-specific metabolic formation of OH-6PPD-Qs. For example, CYP2F3 was detected at comparable abundances across liver, brain and intestine and should thus be excluded as a possible candidate. On the other hand, CYP2K1 was detected in liver >> brain >> intestine and was not detected in the gills, which was highly correlated with the tissue-specific metabolic formation of OH-6PPD-Qs (Figure 3B). By using this strategy, CYP2F2, 2J2, 2K1, and 3A27 were identified as possible candidate isozymes responsible for the hydroxylation of 6PPD-Q. Indeed, in contrast to CYP1A enzymes which have been well-established to hydroxylate the aromatic rings of xenobiotics (*e.g.*, PAHs) in fish,[39,47–49] CYP2K1 from rainbow trout has been reported to regioselectively hydroxylate lauric acid on the (ω-1)-OH position of its alkyl chain.[50] Further studies are warranted to confirm the exact isozymes that are responsible.

Collectively, we herein demonstrated that the hydroxylation of 6PPD-Q in rainbow trout is catalyzed by CYP450 enzymes. With this information, the selective hydroxylation of the C4 carbon on the alkyl side chain of 6PPD-Q became apparent. It has been well established that CYP450 hydroxylation proceeds via the radical mechanism that is colloquially known as "oxygen rebound" where the Fe(IV) oxo complex first abstracts a hydrogen atom to produce a carbon-centered radical (Figure 3C).[51–53] The H-abstraction is the first and rate-limiting step for CYP450 catalyzed hydroxylation. Note that bond dissociation energy (BDE) of a tertiary carbon, (BDE = 403 kJ/mol), is significantly smaller than those of secondary (BDE = 412 kJ/mol) and primary carbon (BDE = 423 kJ/mol).[54] At room temperature, a marginal difference of ~5 kJ/mol can correspond to a rate that is 1,000 to 10,000 times different.[55,56] Moreover, this catalytic mechanism

also accounts for the compound-selective hydroxylation of 6PPD-Q on the alkyl side chain compared to other previously studied PPD-Qs, as 6PPD-Q is the only analogue with a tertiary carbon possessing only alkyl substituents. In contrast, while other PPD-Qs possess tertiary carbons, they are substituted by secondary amino groups. Upon hydroxylation, they will form the unstable hemiaminal functional group that decomposes readily to the corresponding imine or aminal.[54,57,58]

Regioselective toxicity of alkyl-OH-6PPD-Q isomers. Having successfully established that the unique regioselective hydroxylation of 6PPD-Q is due to its C_4 tertiary carbon, we sought to determine the role of C_4-alkyl-OH-6PPD-Q in mediating the toxicity of 6PPD-Q in sensitive salmonid species. Unfortunately, rainbow trout cell lines have not been benchmarked for 6PPD-Q toxicity testing. Indeed, RTG-2, RTgill-W1, and RTL-W1, three commonly used rainbow trout cell lines, were found insensitive to 6PPD-Q.[59,60] Therefore, we decided to use the coho salmon CSE-119 cell line as it has been recently benchmarked as an *in vitro* model for the toxicity testing of 6PPD-Q.[28] As shown in Figure 4A, consistent with previous studies,[28] 6PPD-Q induced the cytotoxicity of CSE-119 cells with an EC_{50} of 17.1 µg/L by using the AlamarBlue assay. The AlamarBlue assay relies on the redox property of a reporter dye, resazurin, which might be confounded considering the antioxidant property of 6PPD.[61] We then employed an orthogonal Neutral Red Assay, which relies on the passive uptake of a red dye (3-amino-7-dimethylamino-2-methyl-phenazine hydrochloride) into healthy cells.[29] Consistent with the results from the AlamarBlue assay, 6PPD-Q also induced the cytotoxicity of CSE-119 cells with an EC_{50} of 16.9 µg/L as measured by Neutral Red (Figure 4B). The two independent bioassays confirmed the CSE-119 cell line as an *in vitro* model for the toxicity testing of 6PPD-Q.

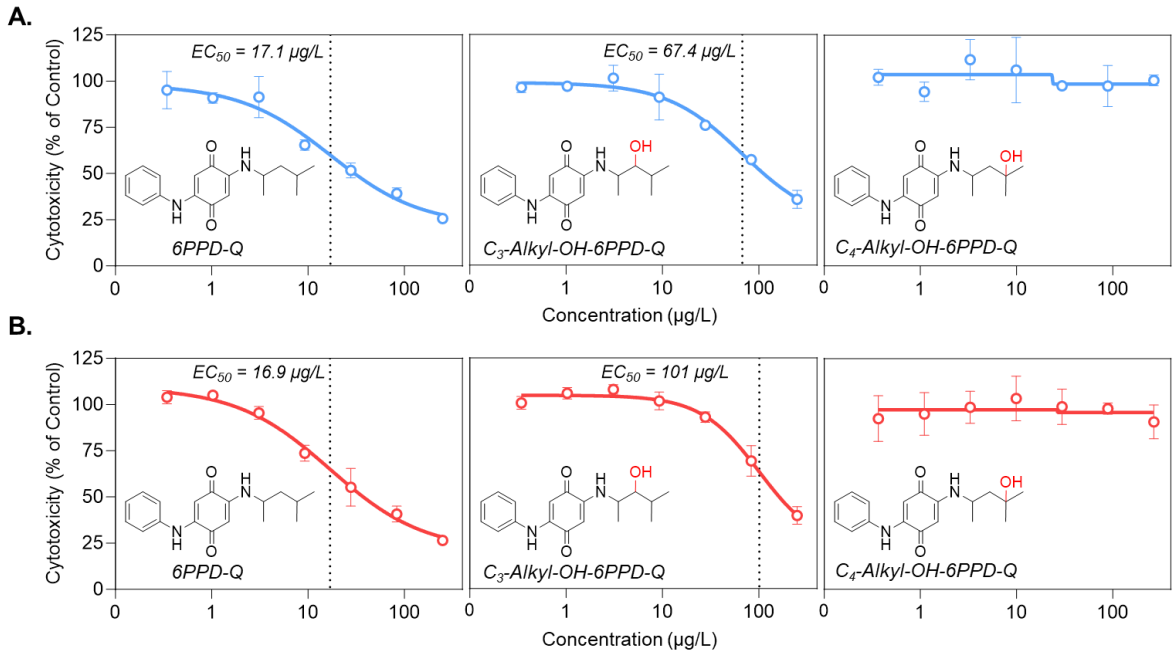

Figure 4. *In vitro* exposure of 6PPD-Q, synthesized C_3-Alkyl-OH-6PPD-Q, and synthesized C_4-Alkyl-OH-6PPD-Q chemical standards to CSE-119. Cytotoxicity measured via both the A) AlamarBlue and B) Neutral Red assays revealed the highly regioselective toxicity of alkyl-OH-6PPD-Q metabolites.

We then proceeded to test the cytotoxicity of C_3- and C_4-alkyl-OH-6PPD-Q by using our synthesized chemical standards. As shown in Figure 4, cytotoxicity was detected for C_3-alkyl-OH-6PPD-Q in both assays, albeit with ~5-fold weaker toxicity than native 6PPD-Q in both Alamar Blue (EC_{50} = 67.4 µg/L) and Neutral Red (EC_{50} = 101 µg/L) assays. This was not completely surprising, as our previous study has already demonstrated that the toxicity of 6PPD-Q is sensitive to even minor structural modifications on its alkyl side chain.[8] We then proceeded to test the toxicity of C_4-alkyl-OH-6PPD-Q and, surprisingly, cytotoxicity was not detected by either Alamar Blue or Neutral Red assay. The lack of toxicity of C_4-alkyl-OH-6PPD-Q was in stark contrast to the toxicity of C_3-alkyl-OH-6PPD-Q, which was only marginally different than that of 6PPD-Q. This was remarkable considering the close proximity of the C_3 and C_4 carbons. The total loss of toxicity upon hydroxylation of the C_4 tertiary carbon of 6PPD-Q highlighted its importance and

demonstrated that this carbon, which amongst the other PPD-Qs uniquely consists of only carbon substituents, is crucial for its toxicity and may account for the structural selectivity observed in our previous studies.[8,9]

Confirmation of the low toxicity of OH-6PPD-Q metabolites formed in liver microsome. While we discovered the total loss of toxicity of C_4-alkyl-OH-6PPD-Q via synthesized standards, this does not necessarily mimic physiologically relevant conditions. For example, it is common for CYP450 enzymes to form enantioselective metabolites which may not be captured by our synthesis.[62–64] To further investigate the toxicity of C_4-alkyl-OH-6PPD-Q under physiologically relevant conditions, we decided to directly isolate the C_4-alkyl-OH-6PPD-Q and other metabolites from rainbow trout liver microsome for toxicity testing. To achieve this, we scaled-up our microsome incubation protocol to achieve a higher concentration of metabolites that would be amenable to toxicity testing. Following a 5 hr incubation of 6PPD-Q in liver microsome, we extracted and exposed the resulting mixture of 6PPD-Q and its metabolite products ("microsome mixture") to CSE-119 cells. As shown in Figure 5A, the cytotoxicity of the microsome extracts decreased after metabolism, compared to native 6PPD-Q. To further confirm this result was not influenced by potential matrix effect from microsome extracts (*e.g.,* by lipids or other cellular components that may have been co-extracted alongside the metabolites)[65], we co-incubated 6PPD-Q with microsome control extracts *(i.e.,* that was not previously incubated with 6PPD-Q). Similar cytotoxicity effects were observed in the absence or presence of the microsome extracts (Figure S12), and therefore the possibility of interference by matrix effects could be excluded.

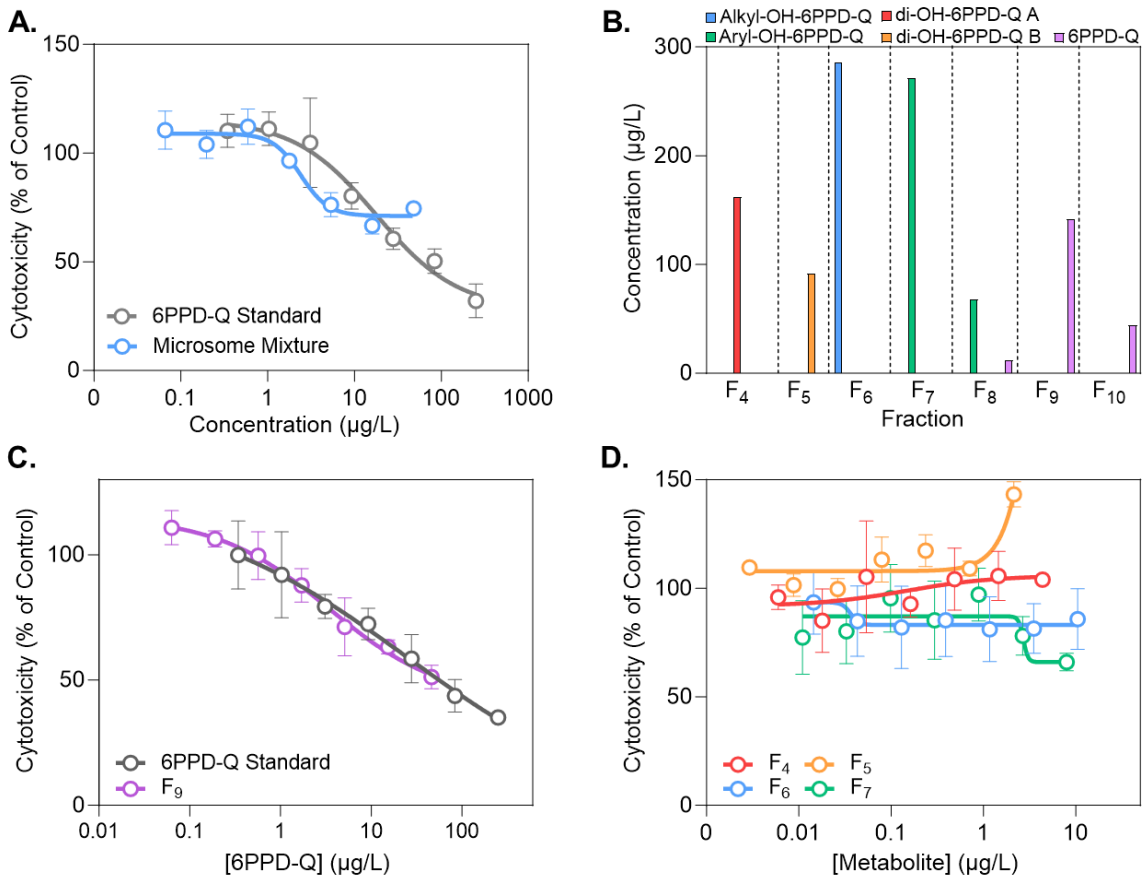

Figure 5. A) *In vitro* exposure of a 6PPD-Q RT liver microsomal incubation mixture to CSE-119 cells in comparison to a 6PPD-Q standard. Microsome concentration is represented as the summed concentration of 6PPD-Q and its metabolites. B) HPLC fractionation of 6PPD-Q and its hydroxylated metabolites from the RT liver microsomal incubation mixture. C) *In vitro* exposure of a 6PPQ-Q chemical standard and 6PPD-Q fractionated from the RT liver microsomal incubation mixture to CSE-119 cells. D) *In vitro* exposure of HPLC fractions of the RT liver microsomal incubation mixture to CSE-119 cells. *In vitro* cytotoxicity results were measured via the AlamarBlue assay.

To further examine the toxicity contributions of individual metabolites, the microsome mixture was then fractionated via HPLC, wherein 5 compounds were separated into different fractions: a di-OH-6PPD-Q product ("di-OH-6PPD-Q A"; F_4), an additional di-OH-6PPD-Q product ("di-OH-6PPD-Q B"; F_5), C_4-alkyl-OH-6PPD-Q (F_6), aryl-OH-6PPD-Q (F_7), and parent 6PPD-Q (F_9) (Figure 5B). The formation of di-OH-6PPD-Qs from 6PPD-Q was previously reported in rainbow trout *in vivo*.[9] While we didn't detect di-OH-6PPD-Q metabolites in our prior microsomal

incubations, their production here was unsurprising as the scaled-up conditions yielded a higher abundance. We then proceeded to expose CSE-119 cells to the F_4,, F_5, F_6, F_7, and F_9 fractions alongside a 6PPD-Q chemical standard to probe their relative toxicities. While comparable toxicities were observed between F_9 and the 6PPD-Q chemical standard (Figure 5C), no dose-dependent toxicity was observed for the fractions containing hydroxylated metabolites (F_{4-7}), including the fraction of C_4-alkyl-OH-6PPD-Q (F_6; Figure 5D). The low toxicity for the fractions of metabolites were further confirmed with the Neutral Red Assay (Figure S13). Together with the toxicity results from synthesized standards and microsome extracts, we concluded that the hydroxylation of 6PPD-Q on the C_4 carbon is likely a detoxication pathway. Future studies are warranted to confirm these results using *in vivo* toxicity testing in rainbow trout and coho salmon fish.

Implications

The unique formation of an alkyl-OH-6PPD-Q metabolite from 6PPD-Q was first reported in our previous study,[8] but its potential role in the toxicity of 6PPD-Q remains unknown. We herein synthesized the chemical standards of alkyl-OH-6PPD-Qs and confirmed C_4-alkyl-OH-6PPD-Q as the predominant alkyl hydroxylated metabolite formed in rainbow trout. Moreover, we discovered that hydroxylation at this C_4 position results in the total loss of toxicity of 6PPD-Q in CSE-119 cells. These results did not support the bioactivation hypothesis that alkyl-OH-6PPD-Q might mediate the toxicity of 6PPD-Q. Instead, hydroxylation on the C_4 carbon appears to be a precisely regulated detoxification pathway for 6PPD-Q, as hydroxylation on the nearby C_3 carbon only minorly influences toxicity. These results were further supported by the formation of C_4-alkyl-OH-6PPD-Q in the liver S9 of arctic char (Figure S14), which was previously reported to be

insensitive to 6PPD-Q.[7] This demonstrated that the production of C_4-alkyl-OH-6PPD-Q is not unique to sensitive species such as rainbow trout. This finding can narrow the focus of future toxicological investigations to native 6PPD-Q, as it, rather than its C_4-alkyl-OH-6PPD-Q metabolite, appears to be the toxic species. Determining the exact binding protein of native 6PPD-Q in future studies is critical to understanding its toxicity mechanism in-depth.

The most striking observation in the current study is the importance of the C_4 tertiary carbon in both the metabolism and toxicity of 6PPD-Q. Our previous study highlighted the importance of the alkyl side chain for the unique toxicity of 6PPD-Q,[8] as toxicity was not observed for other PPD-Qs with distinct alkyl side chains. In the current study, the complete loss of toxicity for C_4-alkyl-OH-6PPD-Q in contrast to C_3-alkyl-OH-6PPD-Q further highlighted that the C_4 tertiary carbon on the alkyl side chain of 6PPD-Q might be the key structural feature for its unique toxicity. To further explore the relevance of the C_4 tertiary carbon of 6PPD-Q, it would be highly interesting for in-depth exploration of structure-toxicity relationship via the synthesis of PPD-Q analogues bearing similar structural features (*i.e.*, tertiary carbon with various alkyl substituents).

Supporting Information Available

The information is available freely via the Internet at http://pubs.acs.org/.

Acknowledgements

This research was supported by National Sciences and Engineering Research Council (NSERC) Discovery Grants and the Ontario Early Researcher Award. The authors acknowledge the support of instrumentation grants from the Canada Foundation for Innovation, the Ontario Research Fund, and the NSERC Research Tools and Instrument Grant. We would like to thank Dr.

John D. Hansen and Dr. Justin B. Greer from the U.S. Geological Survey for kindly sharing the CSE-119 cell line.

Author information

Corresponding authors

Datong Song- Department of Chemistry, University of Toronto, Toronto, Ontario M5S 3H6, Canada;

Hui Peng - Department of Chemistry and School of the Environment, University of Toronto, Toronto, Ontario M5S 3H6, Canada;

Authors

Pranav Nair[#] - Department of Chemistry, University of Toronto, Toronto, Ontario M5S 3H6, Canada;

Holly Barrett[#] - Department of Chemistry, University of Toronto, Toronto, Ontario M5S 3H6, Canada;

Kaylin Tanoto - Department of Chemistry, University of Toronto, Toronto, Ontario M5S 3H6, Canada;

Linna Xie - Department of Chemistry, University of Toronto, Toronto, Ontario M5S 3H6, Canada;

Jianxian Sun - Department of Chemistry, University of Toronto, Toronto, Ontario M5S 3H6, Canada;

Diwen Yang - Department of Chemistry, University of Toronto, Toronto, Ontario M5S 3H6, Canada;

Han Yao - Department of Chemistry, University of Toronto, Toronto, Ontario M5S 3H6, Canada;

[#]Pranav Nair and Holly Barrett contributed equally to this work.

References

(1) Tian, Z.; Zhao, H.; Peter, K. T.; Gonzalez, M.; Wetzel, J.; Wu, C.; Hu, X.; Prat, J.; Mudrock, E.; Hettinger, R.; Cortina, A. E.; Biswas, R. G.; Kock, F. V. C.; Soong, R.; Jenne, A.; Du, B.; Hou, F.; He, H.; Lundeen, R.; Gilbreath, A.; Sutton, R.; Scholz, N. L.; Davis, J. W.; Dodd, M. C.; Simpson, A.; McIntyre, J. K.; Kolodziej, E. P. A Ubiquitous Tire Rubber–Derived Chemical Induces Acute Mortality in Coho Salmon. *Science* **2021**, *371* (6525), 185–189. https://doi.org/10.1126/science.abd6951.

(2) Tian, Z.; Gonzalez, M.; Rideout, C. A.; Zhao, H. N.; Hu, X.; Wetzel, J.; Mudrock, E.; James, C. A.; McIntyre, J. K.; Kolodziej, E. P. 6PPD-Quinone: Revised Toxicity Assessment and Quantification with a Commercial Standard. *Environ. Sci. Technol. Lett.* **2022**, *9* (2), 140–146. https://doi.org/10.1021/acs.estlett.1c00910.

(3) Hiki, K.; Yamamoto, H. The Tire-Derived Chemical 6PPD-Quinone Is Lethally Toxic to the White-Spotted Char *Salvelinus Leucomaenis Pluvius* but Not to Two Other Salmonid Species. *Environ. Sci. Technol. Lett.* **2022**, *9* (12), 1050–1055. https://doi.org/10.1021/acs.estlett.2c00683.

(4) French, B. F.; Baldwin, D. H.; Cameron, J.; Prat, J.; King, K.; Davis, J. W.; McIntyre, J. K.; Scholz, N. L. Urban Roadway Runoff Is Lethal to Juvenile Coho, Steelhead, and Chinook Salmonids, But Not Congeneric Sockeye. *Environ. Sci. Technol. Lett.* **2022**, *9* (9), 733–738. https://doi.org/10.1021/acs.estlett.2c00467.

(5) Foldvik, A.; Kryuchkov, F.; Sandodden, R.; Uhlig, S. Acute Toxicity Testing of the Tire Rubber-Derived Chemical 6PPD-Quinone on Atlantic Salmon (Salmo Salar) and Brown Trout (Salmo Trutta). *Environ. Toxicol. Chem.* **2022**, *41* (Copyright © 2024 American Chemical Society (ACS). All Rights Reserved.; Copyright © 2024 U.S. National Library of Medicine.), 3041–3045. https://doi.org/10.1002/etc.5487.

(6) Foldvik, A.; Kryuchkov, F.; Ulvan, E. M.; Sandodden, R.; Kvingedal, E. Acute Toxicity Testing of Pink Salmon (Oncorhynchus Gorbuscha) with the Tire Rubber-Derived Chemical 6PPD-Quinone. *Environ. Toxicol. Chem.* **2024**, *43* (Copyright © 2024 American Chemical Society (ACS). All Rights Reserved.; Copyright © 2024 U.S. National Library of Medicine.), 1332–1338. https://doi.org/10.1002/etc.5875.

(7) Brinkmann, M.; Montgomery, D.; Selinger, S.; Miller, J. G. P.; Stock, E.; Alcaraz, A. J.; Challis, J. K.; Weber, L.; Janz, D.; Hecker, M.; Wiseman, S. Acute Toxicity of the Tire Rubber-Derived Chemical 6PPD-Quinone to Four Fishes of Commercial, Cultural, and Ecological Importance. *Environ. Sci. Technol. Lett.* **2022**, *9* (Copyright © 2024 American Chemical Society (ACS). All Rights Reserved.), 333–338. https://doi.org/10.1021/acs.estlett.2c00050.

(8) Nair, P.; Sun, J.; Xie, L.; Kennedy, L.; Kozakiewicz, D.; Kleywegt, S.; Hao, C.; Byun, H.; Barrett, H.; Baker, J.; Monaghan, J.; Krogh, E.; Song, D.; Peng, H. Synthesis and Toxicity Evaluation of Tire Rubber-Derived Quinones. June 20, 2023. https://doi.org/10.26434/chemrxiv-2023-pmxvc.

(9) Xie, L.; Yu, Jie; Nair, P.; Sun, J.; Barrett, H.; Meek, O.; Qian, X.; Yang, D.; Kennedy, L.; Kozakiewicz, D.; Hao, C.; Hansen, J. D.; Greer, J. B.; Abbatt, J. P. D.; Peng, H. Structurally Selective Ozonolysis of P-Phenylenediamines and Toxicity in Coho Salmon and Rainbow Trout. April 17, 2024. https://doi.org/10.26434/chemrxiv-2024-jmptn.

(10) Ankley, P. J.; da Silva, F. C. Jr.; Montgomery, D.; Schultz, M.; Ed S. Krol; Hecker, M.; Brinkmann, M. Biotransformation of 6PPD-Quinone In Vitro Using RTL-W1 Cell Line. *Environ. Sci. Technol. Lett.* **2024**, *11* (Copyright © 2024 American Chemical Society (ACS). All Rights Reserved.), 687–693. https://doi.org/10.1021/acs.estlett.4c00342.
(11) Deng, M.; Ji, X.; Peng, B.; Fang, M. In Vitro and In Vivo Biotransformation Profiling of 6PPD-Quinone toward Their Detection in Human Urine. *Environ. Sci. Technol.* **2024**, *58* (21), 9113–9124. https://doi.org/10.1021/acs.est.4c01106.
(12) Song, Z.; Yu, X.; Zhu, M.; Wu, Z.; Fu, Z.; Chen, J. Distinct Species-Specific and Toxigenic Metabolic Profiles for 6PPD and 6PPD Quinone by P450 Enzymes: Insights from In Vitro and In Silico Studies. *Environ. Sci. Technol.* **2024**, *58* (Copyright © 2024 American Chemical Society (ACS). All Rights Reserved.; Copyright © 2024 U.S. National Library of Medicine.), 14994–15004. https://doi.org/10.1021/acs.est.4c03361.
(13) Liao, X.-L.; Chen, Z.-F.; Liu, Q.-Y.; Zhou, J.-M.; Cai, W.-X.; Wang, Y.; Cai, Z. Tissue Accumulation and Biotransformation of 6PPD-Quinone in Adult Zebrafish and Its Effects on the Intestinal Microbial Community. *Environ. Sci. Technol.* **2024**, *58* (Copyright © 2024 American Chemical Society (ACS). All Rights Reserved.; Copyright © 2024 U.S. National Library of Medicine.), 10275–10286. https://doi.org/10.1021/acs.est.4c01409.
(14) Amaro, A. R.; Oakley, G. G.; Bauer, U.; Spielmann, H. P.; Robertson, L. W. Metabolic Activation of PCBs to Quinones: Reactivity toward Nitrogen and Sulfur Nucleophiles and Influence of Superoxide Dismutase. *Chemical research in toxicology* **1996**, *9* (3), 623–629.
(15) McLean, M. R.; Robertson, L. W.; Gupta, R. C. Detection of PCB Adducts by the 32P-Postlabeling Technique. *Chem. Res. Toxicol.* **1996**, *9* (1), 165–171. https://doi.org/10.1021/tx9500843.
(16) Oakley, G. G.; Robertson, L. W.; Gupta, R. C. Analysis of Polychlorinated Biphenyl-DNA Adducts by 32P-Postlabeling. *Carcinogenesis* **1996**, *17* (1), 109–114. https://doi.org/10.1093/carcin/17.1.109.
(17) Robertson, L. W.; Ludewig, G. Polychlorinated Biphenyl (PCB) Carcinogenicity with Special Emphasis on Airborne PCBs. *Gefahrstoffe, Reinhaltung der Luft= Air quality control/Herausgeber, BIA und KRdL im VDI und DIN* **2011**, *71* (1–2), 25.
(18) Espandiari, P.; Glauert, H. P.; Lehmler, H.-J.; Lee, E. Y.; Srinivasan, C.; Robertson, L. W. Polychlorinated Biphenyls as Initiators in Liver Carcinogenesis: Resistant Hepatocyte Model. *Toxicology and Applied Pharmacology* **2003**, *186* (1), 55–62. https://doi.org/10.1016/S0041-008X(02)00018-2.
(19) Lewis, D.; Lake, B. Molecular Modelling of CYP1A Subfamily Members Based on an Alignment with CYP102: Rationalization of CYP1A Substrate Specificity in Terms of Active Site Amino Acid Residues. *Xenobiotica* **1996**, *26* (7), 723–753.
(20) Lewis, D.; Eddershaw, P.; Dickins, M.; Tarbit, M.; Goldfarb, P. Structural Determinants of Cytochrome P450 Substrate Specificity, Binding Affinity and Catalytic Rate. *Chemico-biological interactions* **1998**, *115* (3), 175–199.
(21) Tassaneeyakul, W.; Birkett, D. J.; Veronese, M. E.; McManus, M. E.; Tukey, R. H.; Quattrochi, L. C.; Gelboin, H. V.; Miners, J. O. Specificity of Substrate and Inhibitor Probes for Human Cytochromes P450 1A1 and 1A2. *Journal of Pharmacology and Experimental Therapeutics* **1993**, *265* (1), 401–407.

(22) Zhou, S.-F.; Yang, L.-P.; Zhou, Z.-W.; Liu, Y.-H.; Chan, E. Insights into the Substrate Specificity, Inhibitors, Regulation, and Polymorphisms and the Clinical Impact of Human Cytochrome P450 1A2. *The AAPS journal* **2009**, *11*, 481–494.
(23) Sridhar, J.; Goyal, N.; Liu, J.; Foroozesh, M. Review of Ligand Specificity Factors for CYP1A Subfamily Enzymes from Molecular Modeling Studies Reported To-Date. *Molecules* **2017**, *22* (7), 1143.
(24) Yu, W.; Hjerrild, P.; Jacobsen, K. M.; Tobiesen, H. N.; Clemmensen, L.; Poulsen, T. B. A Catalytic Oxidative Quinone Heterofunctionalization Method: Synthesis of Strongylophorine-26. *Angewandte Chemie* **2018**, *130* (31), 9953–9957.
(25) OECD. Test No. 319B: Determination of in Vitro Intrinsic Clearance Using Rainbow Trout Liver S9 Sub-Cellular Fraction (RT-S9). *OECD Publishing, Paris* **2018**, *OECD Guidelines for the Testing of Chemicals* (Section 3). https://doi.org/10.1787/9789264303232-en.
(26) Dyer, S. D.; Jo Bernhard, M.; Cowan-Ellsberry, C.; Perdu-Durand, E.; Demmerle, S.; Cravedi, J. P. In Vitro Biotransformation of Surfactants in Fish. Part II - Alcohol Ethoxylate (C16EO8) and Alcohol Ethoxylate Sulfate (C14EO2S) to Estimate Bioconcentration Potential. *Chemosphere* **2009**, *76* (7), 989–998. https://doi.org/10.1016/j.chemosphere.2009.04.011.
(27) Zheng, G.; Wan, Y.; Shi, S.; Zhao, H.; Gao, S.; Zhang, S.; An, L.; Zhang, Z. Trophodynamics of Emerging Brominated Flame Retardants in the Aquatic Food Web of Lake Taihu: Relationship with Organism Metabolism across Trophic Levels. *Environmental Science and Technology* **2018**, *52* (8), 4632–4640. https://doi.org/10.1021/acs.est.7b06588.
(28) Greer, J. B.; Dalsky, E. M.; Lane, R. F.; Hansen, J. D. Establishing an In Vitro Model to Assess the Toxicity of 6PPD-Quinone and Other Tire Wear Transformation Products. *Environ. Sci. Technol. Lett.* **2023**, *10* (Copyright © 2024 American Chemical Society (ACS). All Rights Reserved.), 533–537. https://doi.org/10.1021/acs.estlett.3c00196.
(29) Repetto, G.; del Peso, A.; Zurita, J. L. Neutral Red Uptake Assay for the Estimation of Cell Viability/Cytotoxicity. *Nature Protocols* **2008**, *3* (7), 1125–1131. https://doi.org/10.1038/nprot.2008.75.
(30) Han, J.; Wang, S.; Yeung, K.; Yang, D.; Gu, W.; Ma, Z.; Sun, J.; Wang, X.; Chow, C.-W.; Chan, A. W. H.; Peng, H. Proteome-Wide Effects of Naphthalene-Derived Secondary Organic Aerosol in BEAS-2B Cells Are Caused by Short-Lived Unsaturated Carbonyls. *Proc. Natl. Acad. Sci. U.S.A.* **2020**, *117* (41), 25386–25395. https://doi.org/10.1073/pnas.2001378117.
(31) Hall, D. R.; Yeung, K.; Peng, H. Monohaloacetic Acids and Monohaloacetamides Attack Distinct Cellular Proteome Thiols. *Environ. Sci. Technol.* **2020**, *54* (23), 15191–15201. https://doi.org/10.1021/acs.est.0c03144.
(32) Tomy, G. T.; Tittlemier, S. A.; Palace, V. P.; Budakowski, W. R.; Braekevelt, E.; Brinkworth, L.; Friesen, K. Biotransformation of N-Ethyl Perfluorooctanesulfonamide by Rainbow Trout (Onchorhynchus Mykiss) Liver Microsomes. *Environmental Science and Technology* **2004**, *38* (3), 758–762. https://doi.org/10.1021/es034550j.
(33) Stapleton, H. M.; Brazil, B.; Holbrook, R. D.; Mitchelmore, C. L.; Benedict, R.; Konstantinov, A.; Potter, D. In Vivo and in Vitro Debromination of Decabromodiphenyl Ether (BDE 209) by Juvenile Rainbow Trout and Common Carp. *Environmental Science and Technology* **2006**, *40* (15), 4653–4658. https://doi.org/10.1021/es060573x.

(34) Liu, F.; Wiseman, S.; Wan, Y.; Doering, J. A.; Hecker, M.; Lam, M. H. W.; Giesy, J. P. Multi-Species Comparison of the Mechanism of Biotransformation of MeO-BDEs to OH-BDEs in Fish. *Aquatic Toxicology* **2012**, *114–115*, 182–188. https://doi.org/10.1016/j.aquatox.2012.02.024.
(35) Williams, D. E.; Bender, R. C.; Morrissey, M. T.; Selivonchick, D. P.; Buhler, & D. R. *Cytochrome P-450 Isozymes in Salmonids Determined with Antibodies to Purified Forms of P-450 from Rainbow Trout*; 1984; Vol. 14, pp 13–21.
(36) Smith, E. M.; Iftikar, F. I.; Higgins, S.; Irshad, A.; Jandoc, R.; Lee, M.; Wilson, J. Y. In Vitro Inhibition of Cytochrome P450-Mediated Reactions by Gemfibrozil, Erythromycin, Ciprofloxacin and Fluoxetine in Fish Liver Microsomes. *Aquatic Toxicology* **2012**, *109*, 259–266. https://doi.org/10.1016/j.aquatox.2011.08.022.
(37) Gao, G.; Magadan, S.; Waldbieser, G. C.; Youngblood, R. C.; Wheeler, P. A.; Scheffler, B. E.; Thorgaard, G. H.; Palti, Y. A Long Reads-Based *de-Novo* Assembly of the Genome of the Arlee Homozygous Line Reveals Chromosomal Rearrangements in Rainbow Trout. *G3 Genes|Genomes|Genetics* **2021**, *11* (4), jkab052. https://doi.org/10.1093/g3journal/jkab052.
(38) Miranda, C. L.; Henderson, M. C.; Buhler, D. R. Evaluation of Chemicals as Inhibitors of Trout Cytochrome P450s. *Toxicology and Applied Pharmacology* **1998**, *148* (2), 237–244. https://doi.org/10.1006/taap.1997.8341.
(39) Buhler, D. R.; Wang-Buhler, J.-L. Rainbow Trout Cytochrome P450s: Purification, Molecular Aspects, Metabolic Activity, Induction and Role in Environmental Monitoring. *Comparative Biochemistry and Physiology Part C: Pharmacology, Toxicology and Endocrinology* **1998**, *121* (1–3), 107–137. https://doi.org/10.1016/S0742-8413(98)10033-6.
(40) Schenkman, J. B.; Jansson, L. Isolation and Purification of Constitutive Forms of Microsomal Cytochrome P450. In *Cytochrome P450 Protocols*; Humana Press: New Jersey, 1998; Vol. 107, pp 55–68. https://doi.org/10.1385/0-89603-519-0:55.
(41) Ryan, D. E.; Levin, W. Purification and Characterization of Hepatic Microsomal Cytochrome P-450. *Pharmacology & Therapeutics* **1990**, *45* (2), 153–239. https://doi.org/10.1016/0163-7258(90)90029-2.
(42) Miranda, C. L.; Wang, J.-L.; Henderson, M. C.; Buhler', D. R. *Purification and Characterization of Hepatic Steroid Hydroxylases from Untreated Rainbow Trout*; 1989; Vol. 268, pp 227–238.
(43) Matsuo, A. Y. O.; Gallagher, E. P.; Trute, M.; Stapleton, P. L.; Levado, R.; Schlenk, D. Characterization of Phase I Biotransformation Enzymes in Coho Salmon (Oncorhynchus Kisutch). *Comparative Biochemistry and Physiology Part C: Toxicology & Pharmacology* **2008**, *147* (1), 78–84. https://doi.org/10.1016/j.cbpc.2007.08.001.
(44) Chang, T. K. H.; Gonzalez, F. J.; Waxman, D. J. Evaluation of Triacetyloleandomycin, α-Nasymphthoflavone and Diethyldithiocarbamate as Selective Chemical Probes for Inhibition of Human Cytochromes P450. *Archives of Biochemistry and Biophysics* **1994**, *311* (2), 437–442. https://doi.org/10.1006/abbi.1994.1259.
(45) Mohos, V.; Fliszár-Nyúl, E.; Ungvári, O.; Kuffa, K.; Needs, P. W.; Kroon, P. A.; Telbisz, Á.; Özvegy-Laczka, C.; Poór, M. Inhibitory Effects of Quercetin and Its Main Methyl, Sulfate, and Glucuronic Acid Conjugates on Cytochrome P450 Enzymes, and on OATP, BCRP and MRP2 Transporters. *Nutrients* **2020**, *12* (8), 2306. https://doi.org/10.3390/nu12082306.

(46) Östlund, J.; Zlabek, V.; Zamaratskaia, G. In Vitro Inhibition of Human CYP2E1 and CYP3A by Quercetin and Myricetin in Hepatic Microsomes Is Not Gender Dependent. *Toxicology* **2017**, *381*, 10–18. https://doi.org/10.1016/j.tox.2017.02.012.
(47) Scornaienchi, M. L.; Thornton, C.; Willett, K. L.; Wilson, J. Y. Functional Differences in the Cytochrome P450 1 Family Enzymes from Zebrafish (Danio Rerio) Using Heterologously Expressed Proteins. *Archives of Biochemistry and Biophysics* **2010**, *502* (1), 17–22. https://doi.org/10.1016/j.abb.2010.06.018.
(48) Williams, D. E.; Buhler, D. R. BENZO[a]PYRENE-HYDROXYLASE CATALYZED BY PURIFIED ISOZYMES OF CYTOCHROME P-450 FROM B-NAPHTHOFLAVONE-FED RAINBOW TROUT.
(49) Willett, K. L.; Aluru, N. Biotransformation in Fishes. In *Toxicology of Fishes*; CRC Press: Boca Raton, 2024. https://doi.org/10.1201/9781003160694.
(50) Buhler, D. R.; Miranda, C. L.; Deinzer, M. L.; Griffin, D. A.; Henderson, M. C. THE REGIOSPECIFIC HYDROXYLATION OF LAURIC ACID BY RAINBOW TROUT (ONCORHYNCHUS MYKISS) CYTOCHROME P450S.
(51) Guengerich, F. P.; Macdonald, T. L. Chemical Mechanisms of Catalysis by Cytochromes P-450: A Unified View. *Accounts of Chemical Research* **1984**, *17* (1), 9–16.
(52) Ortiz de Montellano, P. R. Hydrocarbon Hydroxylation by Cytochrome P450 Enzymes. *Chemical reviews* **2010**, *110* (2), 932–948.
(53) Meunier, B.; De Visser, S. P.; Shaik, S. Mechanism of Oxidation Reactions Catalyzed by Cytochrome P450 Enzymes. *Chemical reviews* **2004**, *104* (9), 3947–3980.
(54) Smith, M. B. *March's Advanced Organic Chemistry: Reactions, Mechanisms, and Structure*; John Wiley & Sons, 2020.
(55) Gronert, S. An Alternative Interpretation of the C−H Bond Strengths of Alkanes. *J. Org. Chem.* **2006**, *71* (3), 1209–1219. https://doi.org/10.1021/jo052363t.
(56) Benson, S. W. III - Bond Energies. *J. Chem. Educ.* **1965**, *42* (9), 502. https://doi.org/10.1021/ed042p502.
(57) Iwasawa, T.; Hooley, R. J.; Rebek, J. Stabilization of Labile Carbonyl Addition Intermediates by a Synthetic Receptor. *Science* **2007**, *317* (5837), 493–496. https://doi.org/10.1126/science.1143272.
(58) Hooley, R. J.; Iwasawa, T.; Rebek, J. Detection of Reactive Tetrahedral Intermediates in a Deep Cavitand with an Introverted Functionality. *J. Am. Chem. Soc.* **2007**, *129* (49), 15330–15339. https://doi.org/10.1021/ja0759343.
(59) Mahoney, H.; da Silva, F. C. J.; Roberts, C.; Schultz, M.; Ji, X.; Alcaraz, A. J.; Montgomery, D.; Selinger, S.; Challis, J. K.; Giesy, J. P.; Weber, L.; Janz, D.; Wiseman, S.; Hecker, M.; Brinkmann, M. Exposure to the Tire Rubber-Derived Contaminant 6PPD-Quinone Causes Mitochondrial Dysfunction In Vitro. *Environ. Sci. Technol. Lett.* **2022**, *9* (Copyright © 2024 American Chemical Society (ACS). All Rights Reserved.), 765–771. https://doi.org/10.1021/acs.estlett.2c00431.
(60) Dudefoi, W.; Ferrari, B. J. D.; Breider, F.; Masset, T.; Leger, G.; Vermeirssen, E.; Bergmann, A. J.; Schirmer, K. Evaluation of Tire Tread Particle Toxicity to Fish Using Rainbow Trout Cell Lines. *Sci. Total Environ.* **2024**, *912* (Copyright © 2024 American Chemical Society

(ACS). All Rights Reserved.; Copyright © 2024 U.S. National Library of Medicine.), 168933. https://doi.org/10.1016/j.scitotenv.2023.168933.
(61) Kumar, P.; Nagarajan, A.; Uchil, P. D. Analysis of Cell Viability by the alamarBlue Assay. *Cold Spring Harbor Protocols* **2018**, *2018* (6), pdb-prot095489.
(62) Warner, N. A.; Martin, J. W.; Wong, C. S. Chiral Polychlorinated Biphenyls Are Biotransformed Enantioselectively by Mammalian Cytochrome P-450 Isozymes to Form Hydroxylated Metabolites. *Environ. Sci. Technol.* **2009**, *43* (1), 114–121. https://doi.org/10.1021/es802237u.
(63) Uwimana, E.; Ruiz, P.; Li, X.; Lehmler, H.-J. Human CYP2A6, CYP2B6, AND CYP2E1 Atropselectively Metabolize Polychlorinated Biphenyls to Hydroxylated Metabolites. *Environ. Sci. Technol.* **2019**, *53* (4), 2114–2123. https://doi.org/10.1021/acs.est.8b05250.
(64) Uwimana, E.; Maiers, A.; Li, X.; Lehmler, H.-J. Microsomal Metabolism of Prochiral Polychlorinated Biphenyls Results in the Enantioselective Formation of Chiral Metabolites. *Environ. Sci. Technol.* **2017**, *51* (3), 1820–1829. https://doi.org/10.1021/acs.est.6b05387.
(65) Barrett, H.; Sun, J.; Gong, Y.; Yang, P.; Hao, C.; Verreault, J.; Zhang, Y.; Peng, H. Triclosan Is the Predominant Antibacterial Compound in Ontario Sewage Sludge. *Environmental Science & Technology* **2022**. https://doi.org/10.1021/acs.est.2c00406.

767 **TOC**

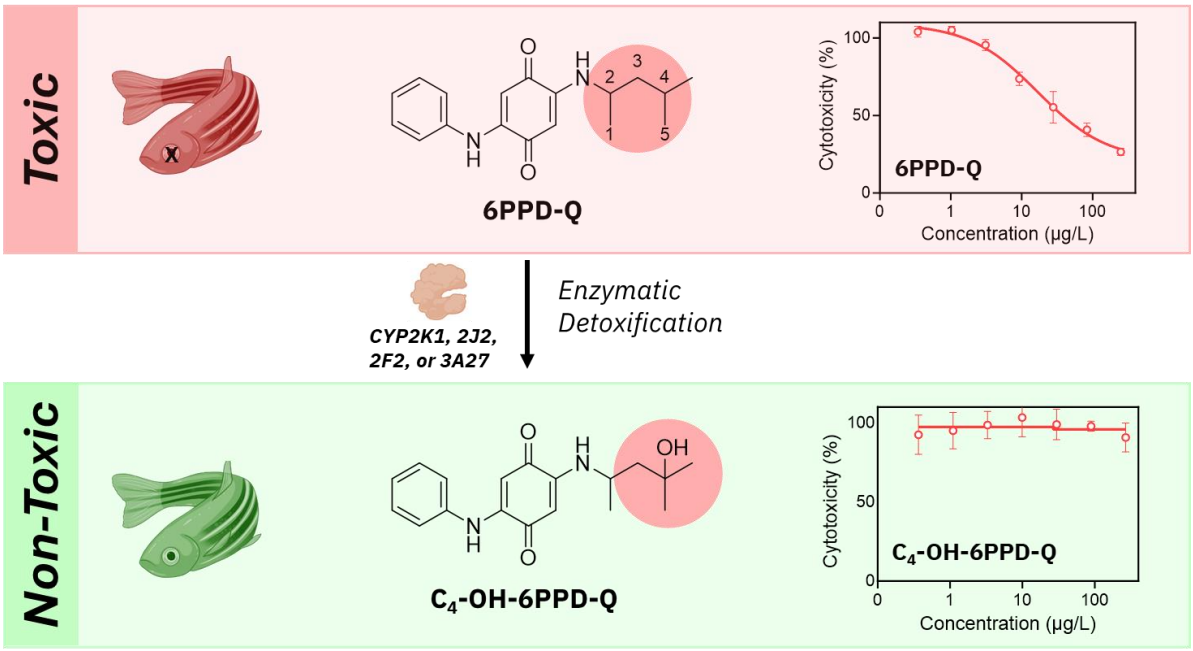

768
769